Inorg. Chem. **1986**, *25*, 983-991 **983**

given in Table IV, are for d^0 complexes where excitation is of the charge-transfer type. In Figure 3 a plot of $\delta(VO_{4-x}S_x^{3-})$ vs. $\delta(MoO_{4-x}S_x^{2-})$ is given, and again an excellent correlation is evident. The relative shiftability yielded by the data is 1.16 for Mo/V. A similar correlation for $^{183}W/^{95}Mo$ oxothio compounds has been reported.[38]

It is also fair to ask what limitations are expected for correlations of this type. There are several. (1) Elements of low atomic number having no low-energy excitations of appropriate transition type will require treatment by the full Ramsey equation. (2) Whenever a compound has an unusual excitation (e.g., $Fe(bpy)_3^{2+}$), there should be a marked deviation from the correlation line; this type of deviation can be useful in predicting excitation symmetries. (3) The influences of medium and charge have been ignored; for the cases herein where $\Delta\delta$ is large this is not a problem, but when $\Delta\delta$ values are small it could influence the degree of correlation.

If the $^{57}Fe/^{59}Co$ chemical shift correlation proves valid, it will allow the prediction of shifts in iron complexes. This should be especially interesting,[39,40] although it has yet to be established that ^{59}Co NMR of cobalt-substituted proteins can be obtained without excessively broad lines (due to slow tumbling and the nuclear quadrupole moment).

Acknowledgment. This work was supported by grants from the National Institutes of Health (Grant No. AM 30145 and AM 01151 and the BRSG Fund of Brown University). We are grateful to Drs. P. J. Domaille and J. G. Jones for helpful discussions, to Dr. J. Van Epp for technical assistance, and to Professor R. G. Kidd for useful suggestions.

Registry No. ^{59}Co, 7440-48-4; ^{57}Fe, 14762-69-7; $[Co(NH_3)_5(py)]\cdot 3CF_3SO_3$, 100447-66-3; $[Co(NH_3)_5(HIm)]\cdot 3CF_3SO_3$, 100447-67-4; $[Co(NH_3)_5(CH_3Im)]\cdot 3CF_3SO_3$, 100466-08-8; $[Co(NH_3)_5(H_2O)]\cdot 3CF_3SO_3$, 69897-22-9; $[Co(TPP)(HIm)]\cdot ClO_4$, 41136-67-8; $[Co(TPP)(CH_3Im)]\cdot ClO_4$, 100447-68-5; $[Co(TPP)(HIm)]\cdot B(Ph)_4$, 100569-86-6; $[Co(TPP)(CH_3Im)]\cdot B(Ph)_4$, 100569-09-3; $[Co(TPP)(HIm)]\cdot BF_4$, 69531-88-0; $[Co(TPP)(CH_3Im)]\cdot BF_4$, 69531-90-4; $[Co(OEP)(HIm)]\cdot BF_4$, 100466-10-2; $[Co(OEP)(CH_3Im)]\cdot BF_4$, 100466-11-3.

---

(38) Gheller, S. F.; Hambley, T. W.; Rodgers, J. R.; Brownlee, R. T. C.; O'Connor, M. J.; Snow, M. R.; Wedd, A. G. *Inorg. Chem.* **1984**, *23*, 2526.

(39) LaMar, G. N.; Dellinger, C. M.; Sankar, S. S. *Biochem. Biophys. Res. Commun.* **1985**, *128*, 628.

(40) Lee, H. C.; Gard, J. K.; Brown, T. L.; Oldfield, E. *J. Am. Chem. Soc.* **1985**, *107*, 4087.

Contribution from the Department of Chemistry,
Brandeis University, Waltham, Massachusetts 02254

Structure, Reactivity, and Electrochemistry of Free-Base β-Oxoporphyrins and Metallo-β-oxoporphyrins

Alan M. Stolzenberg,* Paul A. Glazer, and Bruce M. Foxman

Received September 17, 1985

The free-base and metal complexes of mono- and di-β-oxoporphyrins obtained by hydrogen peroxide oxidation of octaethylporphyrin have been prepared and certain chemical and physicochemical properties investigated. One of these complexes, which are formally analogous to hydroporphyrins, has been proposed to be the essential chromophoric unit of the macrocycle in heme-d_1. The structure of [3,3,7,8,12,13,17,18-octaethyl-2(3*H*)-porphinonato(2−)]nickel, $C_{36}H_{44}N_4ONi$, has been determined by X-ray diffraction. The complex crystallizes in the monoclinic space group $C2/c$ with a = 38.565 (8) Å, b = 14.767 (4) Å, c = 17.327 (5) Å, and β = 102.19 (3)°. There are 12 molecules of the oxoporphyrin per unit cell including four disordered molecules on a special position. The structure has been refined by full-matrix least squares to R = 0.106. The results confirm the structure of the oxoporphyrin macrocycle previously deduced by spectroscopic evidence. The conformations of the two independent molecules are different. The general position molecule is nearly planar, whereas the special position molecule is S_4 ruffled. Both deviate from planarity to a lesser extent than nickel hydroporphyrin complexes. The β-carbonyl group of oxoporphyrins has been found to be remarkably inert. The electrochemical properties of oxoporphyrins are unlike those of hydroporphyrins. The first oxidations of mono- and dioxoporphyrins occur at potentials quite similar to that of octaethylporphyrin. In contrast, the potentials of the first reductions become successively less negative as more carbonyl groups are introduced.

Introduction

The oxidation of octaalkylporphyrins with hydrogen peroxide in acidic media was first investigated by Fisher in the 1930s.[1] The main product had a UV-vis spectrum that resembled those of chlorins and was initially assigned a β,β′-dihydroxychlorin structure, but later studies established that it contained only one oxygen atom.[2] The correct *gem*-dialkyl-β-oxoporphyrin[3] structure was not assigned until 1964.[4,5] The reaction was interpreted as an acid-catalyzed pinacol–pinacolone rearrangement of an initially formed β,β′-dihydroxychlorin,[4,6] a view confirmed by the sulfuric acid-catalyzed rearrangement to identical materials of porphyrins oxidized by OsO_4.[2,4] Later thorough reexaminations of the peroxide reaction system established that reaction did not halt at the mono-β-oxoporphyrin stage.[6-8] All possible isomeric dioxoporphyrin and several isomeric trioxoporphyrins have been isolated from the oxidation of octaethylporphyrin.[8] Structures of octaethylmonooxoporphyrins and -dioxoporphyrins, **5–10**,[9] are depicted in Chart I.

The structure, physical properties, and reactivity of free-base and metallo-β-oxoporphyrins have not been investigated exten-

---

(1) Fisher, H.; Orth, H. "Die Chemie des Pyrrols"; Akademische Verlagsgesselschaft, Leipzig, Germany, 1937; Vol. 2, Part 1, p 269.

(2) Fisher, H.; Pfeiffer, H. *Justus Liebigs Ann. Chem.* **1944**, *556*, 131.

(3) Nomenclature in this area is not well established. We have chosen to refer to the entire class of compounds as β-oxoporphyrins. This choice emphasizes the distinction between oxoporphyrin and hydroporphyrins and better reflects the nomenclature in *Chemical Abstracts*. Earlier literature employs trivial names including oxohydroporphyrin (oxochlorin, dioxoisobacteriochlorin, etc.) and geminiporphyrin mono-, di-, and triketones.

(4) Bonnett, R.; Dolphin, D.; Johnson, A. W.; Oldfield, D.; Stephenson, G. F. *Proc. Chem. Soc., London* **1964**, 371.

(5) Klotmann, G. Dissertation, Technische Universität Braunschweig, 1964.

(6) Bonnett, R.; Dimsdale, M. J.; Stephenson, G. F. *J. Chem. Soc.* C **1969**, 567.

(7) Inhoffen, H. H.; Nolte, W. *Tetrahedron Lett.* **1967**, 2185.

(8) Inhoffen, H. H.; Nolte, W. *Justus Liebigs Ann. Chem.* **1969**, *725*, 167.

(9) We have adopted the numbering scheme of ref 15 to minimize confusion in comparisons with earlier literature.

0020-1669/86/1325-0983$01.50/0 © 1986 American Chemical Society

Chart I

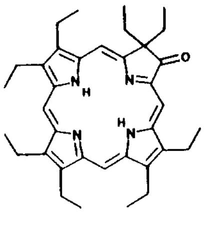

H_2(**5**)

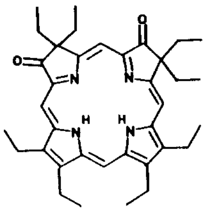

H_2(**6**)

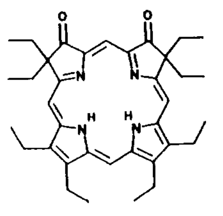

H_2(**7**)

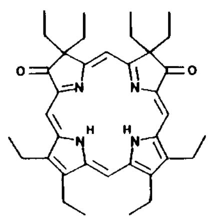

H_2(**8**)

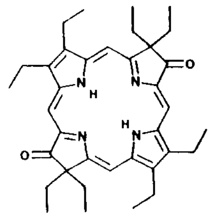

H_2(**9**)

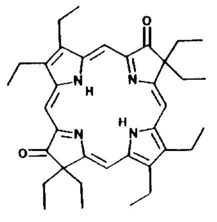

H_2(**10**)

sively. Oxoporphyrins have generally been viewed as analogues of hydroporphyrins, on the basis of the similarity of interruptions in the π systems and the resemblance of the UV–vis spectra of the two classes of macrocycles.[10,11] A few metal complexes of mono-β-oxoporphyrins have been described briefly.[8,12–14] The β-carbonyl group has been reported to react with alkyllithium reagents[8,13] and to form an oxime.[14] Chang has exploited the former reaction in syntheses of dimethyloctaethylisobacteriochlorins[15] and -bacteriochlorins.[16]

A biological role for β-oxoporphyrins has recently emerged. A structure of the dioxoisobacteriochlorin type (adjacent oxidized pyrroline rings) has been proposed for the heme-d_1 prosthetic group isolated from the bacterial nitrite reductase–cytochrome oxidase from *Pseudomonas aeruginosa* and *Pseudomonas denitrificans*.[17] Because of the emerging biological significance of oxoporphyrins and the well-established biological significance of their hydroporphyrin analogues,[18] we have embarked upon an investigation of oxoporphyrin complexes. The properties and reactivity of the more readily accessible mono-β-oxoporphyrins, which should be simpler but typical of the class, have received emphasis. Reported here are the first characterization of an oxoporphyrin complex by X-ray structural means and the first electrochemical data for these complexes. Together with reactivity studies, these data establish that oxoporphyrin and hydroporphyrin complexes are structurally, electronically, and chemically distinct.

Experimental Section

Reagents and Solvents. Benzene, toluene, and THF were dried by distillation from sodium benzophenone ketyl. Acetonitrile (HPLC grade) was dried by distillation from CaH_2. $CDCl_3$ was treated by passage through a column of activated basic alumina. Polarographic grade tetrabutylammonium perchlorate was used as obtained from Eastman Kodak Co. All other reagents and solvents were reagent or HPLC grade and were used without further purification.

Physical Measurements. Absorption spectra were recorded on Cary Model 14 or Perkin-Elmer Model 552 spectrophotometers. Samples were 10^{-5} M in benzene solution unless otherwise noted. Infrared spectra were recorded on a Perkin-Elmer Model 683 spectrophotometer equipped with a data station. Nuclear magnetic resonance spectra were determined on a Varian XL-300 spectrometer; 5 mM $CDCl_3$ solutions were employed unless otherwise noted. Chemical shifts are reported relative to $(CH_3)_4Si$ internal standard. Mass spectra were obtained on a Hewlett-Packard 5985 mass spectrometer. Electrochemical measurements were performed under an argon atmosphere using thoroughly degassed solutions containing 0.1 M tetrabutylammonium perchlorate as the supporting electrolyte with a Princeton Applied Research Model 173 potentiostat-galvanostat, a Model 176 current to voltage converter, and a Model 175 universal programmer. Data were recorded on a Bascom-Turner Model 3120T digital recorder at a digitization rate sufficient to record data points at 2-mV intervals or less. Potentials reported are at a Pt disk electrode and are reported vs. a saturated calomel electrode.

Preparation of Oxoporphyrins. H_2(OEP[19]) was synthesized[20] and was oxidized[8,15] with H_2O_2 in concentrated H_2SO_4 according to literature procedures. The crude reaction products were separated into two fractions by chromatography on a 2 × 4 in. silica gel (Baker 3405) column. The first fraction consisted of all material that could be eluted with CH_2Cl_2 and contained the mono-, di-, and trioxoporphyrins. The second fraction was eluted with pure methanol. The first fraction was rechromatographed essentially according to Chang's procedure.[15] In our hands, yields were somewhat different than reported and varied with the exact reaction conditions and times. Other oxidized porphyrin products were also obtained. A small amount of the orange-brown α,γ-dioxooctaethylporphomethene[21] was isolated. It eluted between unreacted H_2(OEP) and compound **5** with 60:40 methylene chloride/hexane. 2,3-Diethylmaleimide co-eluted with compound **7** and was removed by sublimation. Compounds were purified by recrystallization from CH_2Cl_2/methanol. Separation of compound **8** from **10** and **6** required medium-pressure chromatography on flash grade silica. The quantity of this low-yield compound isolated was insufficient for recrystallization. It was not examined further.

Free Base 5. UV-vis λ_{max}, nm ($10^{-3}\epsilon_M$, cm^{-1}): 404 (108), 487 (5.5), 506 (8.0), 545 (9.9), 584 (4.4), 616 (1.5), 644 (34.2). IR (KBr) ν, cm^{-1}: 3337 (NH), 2966, 2934, 2873 (CH), 1714 (C=O). IR (CH_2Cl_2) ν, cm^{-1}: 3352 (NH), 2973, 2936, 2877 (CH), 1709 (C=O). Fluorescence emission nm: 647, 678 (w), 729 (w). ^1H NMR ($CDCl_3$), δ: −2.90, −2.85 (br, 1 H each, NH); 0.36 (t, 6 H, *gem*-CH_3); 1.81, 1.82, 1.84, 1.85, 1.86, 1.88 (t, 3 H each, CH_3); 2.75, (m, 4 H total, resolves to AB quartet with A = 2.74, B = 2.77, and J_{AB} = 13.6 Hz, *gem*-CH_2); 3.94 (×2), 4.02, 4.06, 4.09 (×2) (quartet, 2 H, CH_2); 9.12, 9.83, 9.86, 9.94 (1 H each, meso-H).

Free Base 6. ^1H NMR ($CDCl_3$), δ: −0.07 (br, 2 H, NH); 0.41, 0.54 (6 H each, *gem*-CH_3); 1.71, 1.72, 1.75, 1.76 (3 H each, CH_3); 2.63 (m, 8 H, 4 overlapping AB quartets, *gem*-CH_2); 3.74, 3.79, 3.85 (×2) (2 H,

---

(10) Scheer, H.; Inhoffen, H. H. In "The Porphyrins"; Dolphin, D., Ed.; Academic Press: New York, 1978; Vol. 2, pp 45–90.

(11) Furhop, J. H. In "Porphyrins and Metalloporphyrins"; Smith, K. M., Ed.; Elsevier: Amsterdam, 1975; p 639.

(12) Inhoffen, H. H.; Gossauer, A. *Justus Liebigs Ann. Chem.* **1969**, *723*, 135.

(13) Inhoffen, H. H.; Muller, N. *Tetrahedron Lett.* **1969**, 3209.

(14) Johnson, A. W.; Oldfield, D. *J. Chem. Soc.* **1965**, 4303.

(15) Chang, C. K. *Biochemistry* **1980**, *19*, 1971.

(16) Barkigia, K. M.; Fajer, J.; Chang, C. K.; Young, R. *J. Am. Chem. Soc.* **1984**, *106*, 6457.

(17) Chang, C. K. *J. Biol. Chem.* **1985**, *260*, 9520.

(18) Stolzenberg, A. M.; Strauss, S. H.; Holm, R. H. *J. Am. Chem. Soc.* **1981**, *103*, 4763.

(19) Abbreviations: H_2(OEP), 2,3,7,8,12,13,17,18-octaethylporphyrin; H_2(OEC), 17,18-dihydro-2,3,7,8,12,13,17,18-octaethylporphyrin (chlorin); H_2(OEiBC), 12,13,17,18-tetrahydro-2,3,7,8,12,13,17,18-octaethylporphyrin (isobacteriochlorin); TMP, 5,10,15,20-tetramethylporphyrin; TMC, 5,10,15,20-tetramethylchlorin; TMiBC, 5,10,15,20-tetramethylisobacteriochlorin.

(20) Wang, C.-B.; Chang, C. K. *Synthesis* **1979**, 548.

(21) Furhop, J. H. *J. Chem. Soc. D* **1970**, 781. Smith, K. M. *J. Chem. Soc., Chem. Commun.* **1971**, 540.

CH$_2$); 8.44, 8.63, 9.28, 9.42 (1 H each, meso-H).

Free Base 7. ^{1}H NMR (CDCl$_3$), δ: -1.64 (br, 2 H, NH); 0.47 (t, 12 H, *gem*-CH$_3$); 1.76, 1.82 (t, 6 H each, CH$_3$); 2.63 (quartet, 8 H, *gem*-CH$_2$); 3.89, 4.01 (quartet, 4 H each, CH$_2$); 8.87 (×2), 9.58, 9.78 (1 H, meso-H).

Free Base 9. ^{1}H NMR (CDCl$_3$), δ: -2.66 (br, 2 H, NH); 0.41 (t, 12 H, *gem*-CH$_3$); 1.81, 1.84 (t, 6 H each, CH$_3$); 2.70 (quartet, 8 H, *gem*-CH$_2$); 3.88, 3.92 (quartet, 4 H each, CH$_2$); 9.06, 9.71 (2 H each, meso-H).

Free Base 10. ^{1}H NMR (CDCl$_3$), δ: -1.87, -1.81 (br, 1 H each, NH); 0.42 (t, 12 H, *gem*-CH$_3$); 1.78, 1.80 (t, 6 H each, CH$_3$); 2.66 (quartet, 8 H, *gem*-CH$_2$); 3.88, 4.00 (quartet, 4 H each, CH$_2$); 8.81, 9.61 (2 H each, meso-H).

Protonation of 5. Solutions of **5** were reacted with nonaqueous acids. Chloroacetic acid was too weak to effect complete conversion to H$_3$(**5**)$^+$. In 4 mM trifluoroacetic acid in benzene, H$_2$(**5**) was converted to H$_3$(**5**)$^+$. H$_4$(**5**)$^{2+}$ was cleanly obtained at 0.1 M trifluoroacetic acid.

(i) H$_3$(5)$^+$. UV–vis $\lambda_{\max}$, nm ($10^{-3}\epsilon_M$, M^{-1} cm^{-1}): 401 (146), 414 (117), 544 (4.8), 569 (6.6), 621 (19.7).

(ii) H$_4$(5)$^{2+}$. UV–vis $\lambda_{\max}$, nm ($10^{-3}\epsilon_M$, M^{-1} cm^{-1}): 414 (134), 536 (3.9), 575 (5.7), 634 (20.7).

Metal Complexes of Compound 5. The Cu, Ni, and Zn complexes of compound **5** were prepared by reaction of the free base and the appropriate metal chloride or acetate (Zn) in DMF.[22] Al and Mg complexes were prepared by reactions with organometallic reagents, as described below.

(a) Cu(5). UV–vis $\lambda_{\max}$, nm ($10^{-3}\epsilon_M$, M^{-1} cm^{-1}): 416 (125), 505 (2.9), 574 (7.5), 619 (34.1). IR (KBr) ν, cm^{-1}: 2966, 2934, 2872 (CH), 1712 (C=O). Mass spectrum (EI), *m/e*: 611 (M$^+$), 582, 567, 552, 537, 522, 306 (M^{2+}). Ratios of (M + 1)$^+$, (M + 2)$^+$, and (M + 3)$^+$ to M$^+$ agreed with those predicted from isotopic abundances.

(b) Ni(5). UV–vis $\lambda_{\max}$, nm ($10^{-3}\epsilon_M$, M^{-1} cm^{-1}): 373 (34.6), 412 (92.1), 545 (6.4), 572 (7.9), 618 (48.0). IR (KBr) ν, cm^{-1}: 2965, 2931, 2865 (CH), 1711 (C=O). ^{1}H NMR (CDCl$_3$), δ: 0.45 (t, 12 H, *gem*-CH$_3$); 1.65, 1.67, 1.70 (×2), 1.73, 1.74 (t, 3 H, CH$_3$); 2.55 (m, 4 H, resolves to AB quartet with $A = 2.54$, $B = 2.57$, and $J_{AB} = 13.6$ Hz, *gem*-CH$_2$); 3.66, 3.72, 3.76 (×4) (quartet, 2 H each, CH$_2$); 8.57, 9.31, 9.38, 9.44 (1 H each, meso-H).

(c) Zn(5). UV–vis $\lambda_{\max}$, nm ($10^{-3}\epsilon_M$, M^{-1} cm^{-1}): 402 (56.2), 418 (170), 572 (9.4), 621 (71.9). IR (KBr) ν, cm^{-1}: 2965, 2933, 2872 (CH), 1709 (C=O, shoulder), 1686 (C=O). ^{1}H NMR (0.1 mM, 19 °C, CDCl$_3$), δ: 0.40 (t, 6 H, *gem*-CH$_3$); 1.83 (m, 18 H, CH$_3$); 2.74 (q, 4 H, *gem*-CH$_2$); 3.93 (m, 12 H, CH$_2$); 8.93, 9.68, 9.77, 9.88 (1 H each, meso-H). Spectra of 5 mM solutions affected by aggregation phenomena.[23] Mass spectrum (EI), *m/e*: 612 (M$^+$), 583, 568, 553, 538, 523, 306 (M^{2+}). Ratios of (M + 1)$^+$ and (M + 2)$^+$ to M$^+$ agreed with those predicted from isotopic abundances.

(d) Al(5)OH. A 20-mg sample of **5** was dissolved in 20 mL of dry benzene and was placed under a nitrogen atmosphere. A 100-μL aliquot of a 2 M solution of trimethylaluminum in toluene was added by syringe. The solution immediately turned kelly green. After being stirred for 5 min, the reaction was quenched with 10 mL of methanol, which was sufficient to loosen the gel that formed. The blue mixture was filtered, and the solvent was removed. The residue was applied to a 1 × 10 cm column of grade 3 alumina. Elution with methylene chloride served to remove a small amount of unreacted **5**. The product was eluted with 1:1 methanol/methylene chloride. Addition of a trace of acetic acid is required to prevent tailing. The solvent was again removed. In order to convert the axial ligand to hydroxide, the residue was redissolved in methylene chloride, treated with 5% aqueous sodium hydroxide, dried with sodium sulfate, and the solvent removed in vacuo without heating. (Formation of the μ-oxo complex [Al(**5**)]$_2$O is facile in vacuo[24] at temperatures as low as 50 °C. This precluded attempts at characterization by mass spectroscopy.) UV–vis $\lambda_{\max}$, nm (A_λ/A_{633}): 380 sh (0.876), 400 sh (1.64), 417 (3.67), 518 (0.075), 543 (0.085), 582 (0.180), 633 (1.000). IR (KBr) ν, cm^{-1}: 3400 br (OH), 2966, 2932, 2872 (CH), 1714 (C=O). ^{1}H NMR (CDCl$_3$, dry), δ: 0.32, 0.54 (v br, 3 H each, *gem*-CH$_3$); 1.80 (m, br, 18 H, CH$_3$); 2.70 (v, br, 4 H, *gem*-CH$_2$); 3.90 (m, 12 H, CH$_2$); 8.86, 9.60, 9.70, 9.83 (br, 1 H each, meso-H).

(e) Mg(5). A 20-mg sample of **5** was dissolved in 20 mL of dry benzene and was placed under a nitrogen atmosphere. Addition by syringe at 50 μL of a 3 M solution of methylmagnesium bromide in diethyl ether resulted in a red solution. Water was added after 5 min to quench the reaction. The blue organic layer was extracted twice with 5 mL of water and dried with sodium sulfate. The solvent was removed to afford a green residue, which was purified by chromatography on a 1 × 5 cm grade 3 alumina column eluted with 2% methanol in methylene chloride. This complex displays some air and light sensitivity upon long-term storage, even as a solid. UV–vis $\lambda_{\max}$, nm (A_λ/A_{625}): 404 sh (1.41), 421 (3.23), 578 (0.155), 596 (0.110), 625 (1.000). Fluorescence emission, nm: 633 (intense enough to be visible under room lights). IR (KBr) ν, cm^{-1}: 2964, 2932, 2872 (CH), 1671 (C=O). The ^{1}H NMR spectrum is extremely broad. Further characterization was not attempted owing to the lability of axial ligands.

(f) Mg(5)(C$_5$H$_5$N)$_2$. The magnesium complex above probably has one or two water or methanol ligands. Dissolution of the above complex in 1% pyridine in benzene results in formation of the pyridine complex, as evidenced by dramatic changes in the ^{1}H NMR spectrum.[23] UV–vis $\lambda_{\max}$, nm (A_λ/A_{627}): 423 (2.34), 578 (0.161), 627 (1.000). Fluorescence emission, nm: 636. ^{1}H NMR (CDCl$_3$ + C$_5$D$_5$N) δ: 0.15 (br, 6 H, *gem*-CH$_3$); 1.81 (m, br, 18 H, CH$_3$); 2.65 (m, br, 4 H, *gem*-CH$_2$); 3.91 (m, br, 12 H, CH$_2$); 8.81, 9.62, 9.74, 9.85 (br, 1 H each, meso-H).

Reduction of the β-Oxo Group of 5. (a) 2-Hydroxy-3,3,7,8,12,13,17,18-octaethylchlorin (11). A 20-mg sample of **5** was dissolved in 25 mL of dry THF, and the resulting solution was stirred under a nitrogen atmosphere. A 250-μL aliquot (7 equiv) of a 1 M solution of lithium triethylborohydride in THF was added by syringe. The color gradually changed to blue green, and a red fluorescence was noted. After 1 h, the reaction was quenched by addition of 500 μL of absolute ethanol. A 200-μL aliquot of water was added after 5 min, and the green solution was stirred for an additional 30 min. After removal of solvent, the residue was redissolved in methylene chloride. The mixture was filtered to remove borate solids, and the filtrate was dried with magnesium sulfate. The solution was concentrated and applied to a 1 × 10 cm grade 3 alumina column. The product was eluted with 1% methanol in methylene chloride. UV–vis $\lambda_{\max}$, nm (A_λ/A_{642}): 391 (3.45), 487 (0.303), 494 (0.311), 519 (0.078), 541 (0.043), 590 (0.084), 615 (0.075), 642 (1.000). IR (KBr) ν, cm^{-1}: 3428 br (OH), 3363 sh (NH), 2965, 2932, 2873 (CH), 1615. IR (CH$_2$Cl$_2$) ν, cm^{-1}: 3604 (OH), 3338 (NH), 3045, 2967, 2931, 2873 (CH), 1614. ^{1}H NMR (CDCl$_3$) δ: -2.58 (br, 2 H, NH); 0.71, 0.97 (t, 3 H each, *gem*-CH$_3$); 1.80 (×2), 1.84 (t, 6 H each, CH$_3$); 2.30, 2.59 (components of AB quartet, 1 H each, $J_{AB} = 14.1$ Hz, *gem*-CH$_2$ cis to OH); 2.55, 2.57 (components of AB quartet, 1 H each, $J_{AB} = 14$ Hz, *gem*-CH$_2$ trans to OH); 2.68 (d, 1 H, D$_2$O exchangeable, OH); 6.53 (d, 1 H, $^3J = 7.6$ Hz to OH proton, β-H); 8.77, 9.18, 9.75, 9.77 (1 H each, meso-H). Mass spectrum (EI), *m/e*: 552 (M$^+$), 534, 523, 276 (M^{2+}). Ratios of (M + 1)$^+$ and (M + 2)$^+$ to M$^+$ agreed with those predicted from isotopic abundances.

(b) Al(11)OH. A 20-mg sample of **5** was dissolved in 10 mL of dry THF and was placed in a Schlenk tube under a nitrogen atmosphere. A 50-mg sample of lithium aluminum hydride was added to 30 mL of dry THF in a second flask. The solution of **5** was transferred under nitrogen by cannula to the flask containing the stirred hydride solution. The color of the solution rapidly turned green, then yellow green, and then brown. After 1 h, the reaction was quenched by addition of 400 μL of ethyl acetate. A 250-μL aliquot of water was added after 5 min, and the solution was exposed to air. Gradually, a precipitate formed, and the color changed to blue. The mixture was filtered, and the solvent was removed. The residue was redissolved in methylene chloride, treated with 5% aqueous sodium hydroxide, dried with magnesium sulfate, and filtered. The solution was concentrated and applied to a 2 × 12 cm grade 3 alumina column. Elution with methylene chloride permitted isolation of trace quantities of a green and a pink material (unidentified), but the bulk of the material moved exceedingly slowly. A blue green (major) and a powder blue (minor) fraction (stereoisomers—see text) were cleanly separated by elution with 1% methanol in methylene chloride. (i) Major product. UV–vis $\lambda_{\max}$, nm (A_λ/A_{627}): 391 (2.88), 399 (3.21), 502 (0.142), 540 (0.146), 590 (0.255), 627 (1.000). IR (KBr) ν, cm^{-1}: 3428 br (OH), 2965, 2931, 2871 (CH), 1634. IR (CH$_2$Cl$_2$) ν, cm^{-1}: 3049, 2967, 2932, 2872 (CH), 1637. ^{1}H NMR (CDCl$_3$) δ: 0.73, 0.91 (br, 3 H, *gem*-CH$_3$); 1.75 (m, br, 18 H, CH$_3$); 2.33 (m, br, about 4 H, *gem*-CH$_2$ and OH); 3.70 (m, br, 12 H, CH$_2$); 4.43 (br, 1 H, β-H); 8.34, 8.56, 9.46, 9.48 (br, 1 H, meso-H). (ii) Minor product. UV–vis $\lambda_{\max}$, nm (A_λ/A_{632}): 392 (3.70), 401 (3.78), 505 (0.193), 543 (0.161), 595 (0.312), 632 br (1.000).

X-ray Structure Determination. A suitable crystal of Ni(**5**) was obtained by slow diffusion of a layer of methanol into a chloroform solution of the complex. Preliminary Weissenberg photographs exhibited systematic absences ($h0l$, $l = 2n + 1$; hkl, $h + k = 2n + 1$) and symmetry indicative of either space group Cc or $C2/c$. Most operations on the Syntex P2$_1$ diffractometer and XTL structure determination system were carried out as described previously;[25,26] other operations are described

---

(22) Adler, A. D.; Longo, F. R.; Kampas, F.; Kim, J. *J. Inorg. Nucl. Chem.* **1970**, *32*, 2443.

(23) Stolzenberg, A. M., submitted for publication in *Inorg. Chem.*

(24) Inhoffen, H. H.; Buchler, J. W. *Tetrahedron Lett.* **1968**, 2057.

(25) Foxman, B. M. *Inorg. Chem.* **1978**, *17*, 1932–1938.

Table I. Data for the X-ray Diffraction Study of Ni(**5**)

(A) Crystal Data

cryst system: monoclinic
space group: $C2/c$
$a = 38.565\ (8)$ Å
$b = 14.767\ (4)$ Å
$c = 17.327\ (5)$ Å
$\beta = 102.19\ (3)°$
$V = 9645.1$ Å^3
$Z = 12$
cryst size: 0.32 × 0.32 × 0.10 mm
fw = 607.5
$\rho_{calcd} = 1.25$ g/cm^3
$\rho_{obsd}{}^a = 1.23\ (1)$ g/cm^3
$\mu = 6.4$ cm^{-1} (Mo Kα)

cell const determin: 12 pairs of $\pm(hkl)$ and refined 2θ, ω, and χ values in the range $20° < |2\theta| < 22°$ (λ(Mo Kα) = 0.71073 Å)

(B) Measurement of Intensity Data

radiation: Mo Kα, graphite monochromator
reflcns measd: $+h$, $+k$, $\pm l$ (to $2\theta = 38°$)
scan type, speed: ω, 2.93–5.33°/min
scan range: 1° with a 1.4° displacement in ω for bkgd from Kα position
no. of reflcns measd: 3965; 3887 in unique set
std reflcns: 041, 006, 602; period 150; variation $\leqslant 3\sigma(I)$ for each
abs corr: empirical; transmissn factors 0.888–1.000
data reduction: as before[b]
statistical information:[c] $R_s = 0.044$; $R_{av} = 0.021$ ($0kl$ reflcns)

(C) Refinement

refinement[d] with 2356 data for which $F > 3.92\ \sigma(F)$
weighting of reflcns: as before,[b] $p = 0.035$
full-matrix least squares: anisotropic temperature factors for Ni atom; isotropic temperature factors for all other atoms; $R = 0.106$; $R_w = 0.152$; SDU = 2.74
structure factor calcn, all 3887 unique data: $R = 0.171$, $R_w = 0.180$
final difference map: 4 peaks 0.7–1.15 e$^-$/Å^3 near C(21′), C(23′), and C(29′); other peaks random, <0.6 e^{-1}/Å^3
weighting scheme anal.: no systematic dependence on magnitude of $|F_o|$, $(\sin\theta)/\lambda$, or indices

[a] Determined by neutral buoyancy in aqueous CsCl. [b] Foxman, B. M.; Goldberg, P. L.; Mazurek, H. *Inorg. Chem.* **1981**, *20*, 4381. [c] $R_s = \sum(\sigma|F_o|)/\sum|F_o|$; $R_{av} = \sum(|I - I_{av}|)/\sum|I|$. [d] $R = \sum||F_o| - |F_c||/\sum|F_o|$; $R_w = \{\sum[|F_o| - |F_c|]^2/\sum w|F_o|^2\}^{1/2}$; SDU = $\{\sum_w[|F_o| - |F_c|]^2/(m - n)\}$, where m (=2356) is the number of observations and n (=259) is the number of parameters.

below. Details of the structure analysis, in outline form, are presented in Table I.

All crystals used in this study had poor diffraction properties. The maximum Bragg angle observed was about $\theta = 20°$ on all film and diffractometer measurements; the data collection was limited accordingly. The structure was solved and refined in space group $C2/c$. There was no evidence (statistics, Patterson function, or difference Fourier maps) for space group Cc being the correct choice. As implied by density measurements ($Z = 12$), the solution established the presence of one molecule on a general position and a second molecule on a twofold axis. Since the molecule cannot possess C_2 symmetry, it must be disordered. It was expected that gross structural and stereochemical characterization of the disordered molecule could be obtained from the refinement, and that these results would be consistent with those obtained for the ordered molecule. As discussed below, this is indeed the case. Two N atoms and the Ni atom of the disordered molecule lie on a crystallographic twofold axis, as can be observed from the coordinates (Table II). Owing to the low precision of the data, it was not possible to completely describe the disorder, which apparently involves interchange of the carbonyl and *gem*-diethyl groups by the twofold axis. Finally, although several disorder models were attempted, it was not possible to obtain a satisfactory description of the positions of the methyl carbon atoms of the *gem*-diethyl group or the methyl carbon atom attached to C(29′). Nevertheless, the ordered and disordered molecules are nearly identical, as discussed below, and it seems quite likely that our description of the disorder is satisfactory.

Results and Discussion

Hydrogen peroxide oxidation of H_2(OEP) in concentrated sulfuric acid affords a crude product mixture that contains numerous unidentified porphyrin degradation products in addition to the oxoporphyrins. The latter are obtained in pure form by chromatography in individual yields based upon H_2(OEP) ranging from tenths of a percent to about 20%. The high-field spectra of free-base oxoporphyrins reported here agree well with the original data[8] obtained at 100 MHz and at 5-10 times greater concentration, but additional features may be discerned.

Table II. Positional Parameters and Standard Deviations of the Non-Hydrogen Atoms of Ni(**5**)

atom	*x*	*y*	*z*
Ni(1)	0.24156 (8)	0.0628 (2)	0.0911 (2)
O(1)	0.1018 (5)	0.1356 (12)	0.0202 (10)
N(1)	0.1889 (4)	0.0490 (12)	0.0668 (9)
N(2)	0.2464 (5)	−0.0701 (12)	0.0945 (10)
N(3)	0.2935 (4)	0.0750 (11)	0.1091 (9)
N(4)	0.2368 (5)	0.1949 (11)	0.0913 (10)
C(1)	0.1646 (6)	0.121 (2)	0.0571 (14)
C(2)	0.1283 (7)	0.085 (2)	0.0369 (14)
C(3)	0.1302 (6)	−0.013 (2)	0.0361 (14)
C(4)	0.1693 (6)	−0.030 (2)	0.0591 (13)
C(5)	0.1833 (6)	−0.1139 (15)	0.0699 (13)
C(6)	0.2182 (6)	−0.1333 (15)	0.0873 (13)
C(7)	0.2350 (7)	−0.222 (2)	0.0990 (14)
C(8)	0.2693 (6)	−0.215 (2)	0.1095 (13)
C(9)	0.2777 (6)	−0.1199 (15)	0.1069 (12)
C(10)	0.3110 (6)	−0.082 (2)	0.1138 (12)
C(11)	0.3184 (5)	0.0068 (14)	0.1174 (12)
C(12)	0.3530 (6)	0.042 (2)	0.1296 (13)
C(13)	0.3503 (6)	0.133 (2)	0.1306 (13)
C(14)	0.3126 (5)	0.1551 (15)	0.1184 (12)
C(15)	0.2988 (6)	0.243 (2)	0.1168 (13)
C(16)	0.2631 (6)	0.2592 (14)	0.1053 (12)
C(17)	0.2498 (6)	0.3501 (14)	0.1043 (12)
C(18)	0.2154 (6)	0.3400 (15)	0.0893 (12)
C(19)	0.2061 (6)	0.2435 (15)	0.0813 (13)
C(20)	0.1724 (6)	0.211 (2)	0.0626 (13)
C(21)	0.1084 (9)	−0.053 (2)	0.091 (2)
C(22)	0.1206 (10)	−0.020 (3)	0.176 (2)
C(23)	0.1123 (7)	−0.049 (2)	−0.042 (2)
C(24)	0.1291 (8)	−0.015 (2)	−0.109 (2)
C(25)	0.2135 (7)	−0.308 (2)	0.102 (2)
C(26)	0.2049 (8)	−0.322 (2)	0.183 (2)
C(27)	0.2976 (7)	−0.291 (2)	0.1206 (15)
C(28)	0.3166 (8)	−0.297 (2)	0.209 (2)
C(29)	0.3865 (6)	−0.012 (2)	0.1387 (14)
C(30)	0.3993 (7)	−0.041 (2)	0.225 (2)
C(31)	0.3799 (7)	0.209 (2)	0.141 (2)
C(32)	0.3902 (8)	0.243 (2)	0.225 (2)
C(33)	0.2720 (6)	0.433 (2)	0.1202 (13)
C(34)	0.2826 (7)	0.456 (2)	0.210 (2)
C(35)	0.1875 (6)	0.418 (2)	0.0849 (13)
C(36)	0.1769 (6)	0.433 (2)	0.1660 (14)
Ni(2)	0.5000 (0)	−0.0256 (3)	0.2500 (0)
O(1′)	0.5265 (12)	−0.373 (3)	0.337 (3)
N(1′)	0.5000 (0)	−0.163 (2)	0.2500 (0)
N(2′)	0.5220 (4)	−0.0251 (12)	0.3619 (10)
N(3′)	0.5000 (0)	0.107 (2)	0.2500 (0)
C(3′)	0.5134 (8)	−0.315 (2)	0.288 (2)
C(4′)	0.5180 (7)	−0.215 (2)	0.313 (2)
C(5′)	0.5352 (6)	−0.188 (2)	0.3797 (15)
C(6′)	0.5362 (6)	−0.101 (2)	0.4086 (15)
C(7′)	0.5502 (6)	−0.067 (2)	0.4868 (14)
C(8′)	0.5431 (6)	0.018 (2)	0.4913 (14)
C(9′)	0.5267 (6)	0.047 (2)	0.4135 (14)
C(10′)	0.5190 (6)	0.135 (2)	0.3940 (15)
C(11′)	0.5075 (6)	0.163 (2)	0.3177 (15)
C(12′)	0.5037 (9)	0.263 (2)	0.288 (2)
C(21′)	0.547 (2)	−0.358 (4)	0.262 (4)
C(23′)	0.494 (2)	−0.371 (4)	0.341 (4)
C(25′)	0.5683 (8)	−0.135 (2)	0.554 (2)
C(26′)	0.6077 (8)	−0.152 (2)	0.549 (2)
C(27′)	0.5517 (7)	0.083 (2)	0.564 (2)
C(28′)	0.5866 (8)	0.137 (2)	0.563 (2)
C(29′)	0.5140 (9)	0.350 (2)	0.352 (2)

Unlike the low-field spectra, nearly all of the inequivalencies predicted on the basis of symmetry are observable at high field. For example, decoupling experiments with H_2(**5**) permit assignments of the chemical shifts for each of the six methyl groups in the nonoxidized portion of the macrocycle. In addition, the diastereotopic methylene protons of the *gem*-diethyl groups[27]

---

(26) Foxman, B. M.; Mazurek, H. *Inorg. Chem.* **1979**, *18*, 113–116.

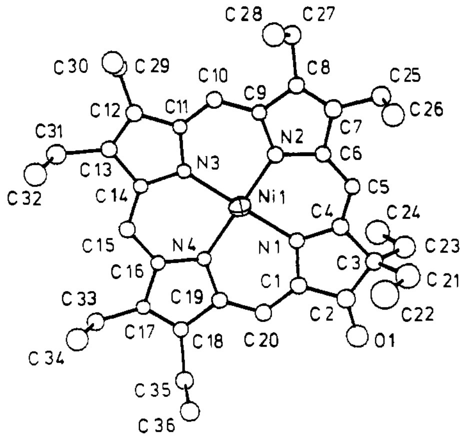

Figure 1. ORTEP diagram of the general position molecule of [3,3,7,8,12,13,17,18-octaethyl-2(3*H*)-porphinonato(2−)]nickel, showing 50% probability ellipsoids for Ni. C and N atoms were refined with isotropic temperature factors, which have been reduced by half for clarity in this figure and in Figure 2.

appear as a narrow "doublet" of a quartet, which collapses to the expected AB quartet upon irradiation of the *gem*-diethyl methyl protons. The 0.03 ppm chemical shift difference between the two diastereotopic protons establishes that they are nearly isochronous despite the expected effects of the diamagnetic anisotropy of the adjacent carbonyl group. The near isochrony of the methylene protons on the oxidized ring(s) appears to be general in free-base oxoporphyrins.

The two N–H protons of $H_2(\mathbf{5})$ and $H_2(\mathbf{10})$ are inequivalent in any reasonable tautomeric structure of these complexes. Tautomeric exchange of these protons is sufficiently slow that two separate resonances can be observed at high field. Behavior of this type has been observed for chlorin e_6 trimethyl ester,[28] but not for the simple chlorin H_2(OEC). Only one N–H resonance is observed for $H_2(\mathbf{9})$, which can have as high as C_{2h} symmetry, and for the isobacteriochlorin-like dioxoporphyrin isomers $H_2(\mathbf{6})$ and $H_2(\mathbf{7})$. The N–H protons of $H_2(\mathbf{6})$ are inequivalent by symmetry, but the downfield shift of these previously unobserved protons to −0.07 ppm[29] establishes considerable reduction in the aromaticity of this complex relative to the other oxoporphyrins. In turn, this may make accessible several tautomeric structures (possibly with small chemical shift differences between the N–H protons) and/or accelerate the rate of tautomeric exchange. Both could lead to coalescence of the N–H resonances. In this light, it is interesting that true isobacteriochlorins have two individual tautomeric structures that rapidly equilibrate.[15] That the appearance of the N–H proton resonance is sensitive to subtle structural changes is evident from the observation of two peaks for 13,17-bis[2-(methoxycarbonyl)ethyl]-3,3,7,8,12,18-hexamethyl-2-oxoporphinone but only one for the 2,2-methyl-3-oxo isomer.[30]

Reactivity at the Oxoporphyrin Core. $H_2(\mathbf{5})$ is sequentially protonated to the cation $H_3(\mathbf{5})^+$ and the dication $H_4(\mathbf{5})^{2+}$ upon reaction with strong acid. Unlike the hydroporphyrins H_2(OEC)[31] and H_2(OEiBC),[32] the oxoporphyrin $H_2(\mathbf{5})$ is not converted completely to the cation $H_3(\mathbf{5})^+$ by reaction with chloroacetic acid in benzene. The lower basicity of oxoporphyrins relative to hydroporphyrins is consistent with the results of the electrochemical experiments discussed below.

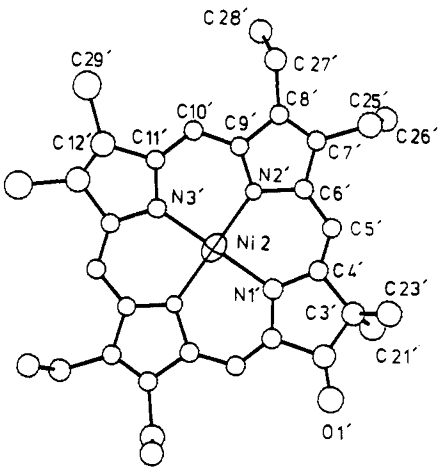

Figure 2. ORTEP diagram for the special position molecule of [3,3,7,8,12,13,17,18-octaethyl-2(3*H*)-porphinonato(2−)]nickel. This is an idealized view of the disordered molecule; a twofold axis passes through Ni(2), N(1′), and N(3′). Note that only *one* of the "doubled" carbonyl oxygen atoms and pair of methylene groups are shown.

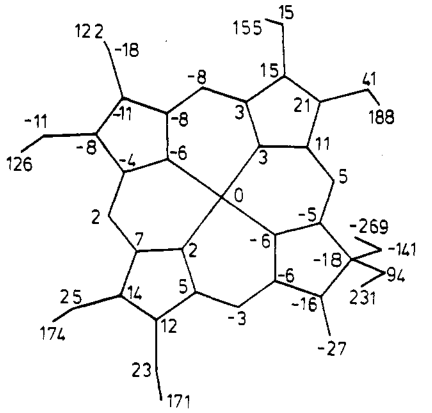

Figure 3. Deviations (Å × 10^2) from the least-squares plane of the 24 macrocycle atoms for the general position molecule. Typical esd's are 0.016 for N and O atoms and 0.02 for C atoms.

Metal complexes of $H_2(\mathbf{5})$ can be prepared by the methods appropriate for porphyrins. The UV–vis spectra of the metal complexes are closer in appearance to spectra of typical metalloporphyrins and -hydroporphyrins than are the spectra of the free-base oxoporphyrins. The ^{1}H NMR spectrum of Ni(**5**) is unremarkable. The spectrum of Al(**5**)OH is often broadened by hydrogen bonding of the axial OH ligand to the carbonyl group of a second molecule and by partial conversion to the μ-oxo complex $[\mathrm{Al}(\mathbf{5})]_2\mathrm{O}$.[24] Spectra of Zn(**5**) and Mg(**5**) are severely broadened[33] by aggregation phenomena involving coordination of the carbonyl group of one molecule to the metal ion of the second.[23] The expected spectra of these complexes can be obtained in dilute solution or in the presence of pyridine, respectively.

Structure of Ni(5). Ni(**5**) crystallizes in space group *C*2/*c* with *Z* = 12. Eight molecules occupy a general position and four disordered molecules occupy special positions 4e on a twofold axis. The precision of the structure determination is limited, owing to problems arising from the disorder and the limited data set (see Experimental Section). The ordered and disordered molecules are shown in Figures 1 and 2, respectively. These results confirm the oxoporphyrin structure assigned upon the basis of spectroscopic evidence. All macrocycle bond lengths and angles in the molecules are indistinguishable from those found in the appropriate regions of typical nickel porphyrin complexes[34] and nickel chlorin com-

---

(27) Replacement of one of these protons with a deuteron creates two chiral centers. It induces chirality at the methylene carbon and destroys the mirror plane passing through the quaternary carbon that relates the two geminal ethyl groups.

(28) Scheer, H.; Katz, J. J. In "Porphyrins and Metalloporphyrins"; Smith, K. M., Ed.; Elsevier Amsterdam, 1975; p 405.

(29) The assignment of this N–H resonance is confirmed by Chang in ref 17.

(30) Chang, C. K.; Sotiriou, C. *J. Org. Chem.* **1985**, *50*, 4989.

(31) Stolzenberg, A. M.; Spreer, L. O.; Holm, R. H. *J. Am. Chem. Soc.* **1980**, *102*, 364.

(32) Stolzenberg, A. M. Ph.D. Thesis, Stanford University, 1980.

(33) The ^{1}H NMR spectrum of Zn(**5**) is very broad at 90 MHz, but is reasonably sharp at 300 MHz. Mg(**5**) is broad at all field strengths.

(34) Scheidt, W. R. In "The Porphyrins"; Dolphin, D., Ed.; Academic Press: New York, **1978**; Vol. 3, pp 463–511.

Table III. Selected Bond Lengths (Å) and Angles (deg) of Ni(**5**)[a]

(a) Ni–N Bond Lengths and Angles			
(i) General Position Molecule			
Ni(1)–N(1)	1.994 (18)	N(1)–Ni(1)–N(2)	89.4 (7)
Ni(1)–N(2)	1.972 (18)	N(2)–Ni(1)–N(3)	90.0 (7)
Ni(1)–N(3)	1.971 (17)	N(3)–Ni(1)–N(4)	90.0 (7)
Ni(1)–N(4)	1.959 (16)	N(1)–Ni(1)–N(4)	90.6 (7)
(ii) Special Position Molecule			
Ni(2)–N(1′)	2.030 (29)	N(1′)–Ni(2)–N(2′)	90.2 (7)
Ni(2)–N(2′)	1.945 (17)	N(2′)–Ni(2)–N(3′)	89.8 (7)
Ni(2)–N(3′)	1.960 (27)	N(1′)–Ni(2)–N(3′)	179.9 (7)
(b) Bond Lengths and Angles Associated with the Pyrrolidinone Ring			
(i) General Position Molecule			
N(1)–C(1)	1.41 (3)	N(1)–C(1)–C(2)	110 (2)
N(1)–C(4)	1.38 (3)	C(2)–C(1)–C(20)	124 (2)
C(1)–C(2)	1.47 (4)	C(1)–C(2)–C(3)	108 (2)
C(1)–C(20)	1.36 (3)	C(1)–C(2)–O(1)	122 (2)
C(2)–C(3)	1.45 (4)	C(3)–C(2)–O(1)	129 (2)
C(2)–O(1)	1.25 (3)	C(2)–C(3)–C(4)	103 (2)
C(3)–C(4)	1.50 (4)	C(2)–C(3)–C(21)	110 (2)
C(3)–C(21)	1.53 (4)	C(2)–C(3)–C(23)	111 (2)
C(3)–C(23)	1.49 (4)	C(4)–C(3)–C(21)	115 (2)
C(4)–C(5)	1.35 (3)	C(4)–C(3)–C(23)	115 (2)
C(21)–C(22)	1.51 (5)	C(3)–C(4)–C(5)	123 (2)
C(23)–C(24)	1.53 (4)	C(3)–C(4)–N(1)	113 (2)
		C(21)–C(3)–C(23)	103 (2)
		C(1)–N(1)–C(4)	107 (2)
		N(1)–C(1)–C(20)	127 (2)
		N(1)–C(4)–C(5)	125 (2)
(ii) Special Position Molecule			
N(1′)–C(4′)	1.39 (3)	N(1′)–C(4′)–C(3′)	107 (2)
C(3′)–C(3′)*	1.48 (4)	N(1′)–C(4′)–C(5′)	129 (2)
C(3′)–C(4′)	1.55 (4)	C(3′)–C(4′)–C(5′)	124 (2)
C(3′)–C(21′)	1.58 (7)	C(4′)–C(3′)–O(1′)	117 (3)
C(3′)–C(23′)	1.54 (7)	C(3′)*–C(3′)–O(1′)	136 (3)
C(3′)–O(1′)	1.23 (5)	C(3′)*–C(3′)–C(4′)	105 (2)
C(4′)–C(5′)	1.26 (4)	C(3′)*–C(3′)–C(21′)	102 (3)
		C(3′)*–C(3′)–C(23′)	101 (3)
		C(4′)–C(3′)–C(21′)	115 (3)
		C(4′)–C(3′)–C(23′)	112 (3)
		C(21′)–C(3′)–C(23′)	118 (4)
		C(4′)*–N(1′)–C(4′)	114 (2)

[a] An asterisk denotes atoms related by the twofold axis.

Table IV. Average Values of Bond Lengths (Å) and Angles (deg) of the Nonoxidized Portion of Ni(**5**)[a]

	general position	special position
C_a–N	1.38 (3)	1.40 (3)
C_a–C_m	1.37 (3)	1.37 (4)
C_a–C_b	1.45 (3)	1.43 (3)
C_b–C_b	1.32 (3)	1.30 (4)
C_b–CH_2	1.53 (3)	1.56 (4)
CH_2–CH_3	1.54 (4)	1.56 (4)
Ni–N–C_a	127 (1)	127 (1)
C_a–N–C_a	106 (2)	108 (2)
N–C_a–C_m	126 (2)	125 (2)
N–C_a–C_b	109 (2)	108 (2)
C_m–C_a–C_b	125 (2)	126 (2)
C_a–C_b–C_b	108 (2)	109 (2)
C_a–C_b–CH_2	124 (2)	122 (2)
C_a–C_m–C_a	124 (2)	124 (2)
C_b–C_b–CH_2	128 (2)	129 (2)
C_b–CH_2–CH_3	111 (2)	110 (2)

[a] Esd's given are for an individual measurement.

plexes.[35] Selected bond lengths and angles (oxidized pyrrole ring and coordination about nickel) are given in Table III. Average values of bond lengths and angles for the nonoxidized portion of the molecules are presented in Table IV.

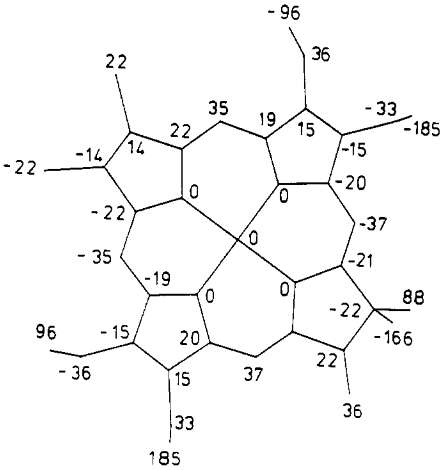

Figure 4. Deviations (Å × 10^2) from the least-squares plane of the 24 macrocycle atoms for the special position molecule. Typical esd's are 0.02 for N and O atoms and 0.03 for C atoms.

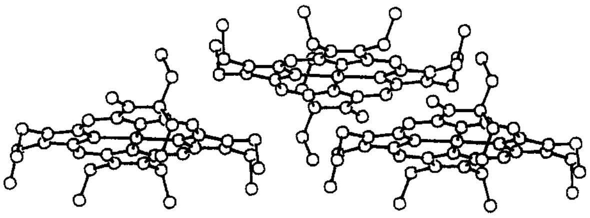

Figure 5. Partial packing diagram of the general position molecules. The upper molecule (x, y, z) is partially overlapped by two symmetry-related molecules ($-x$, $-y$, $-z$ and $-x$, $1 - y$, $-z$).

The deviations of all atoms from the mean macrocycle planes are given for the ordered and disordered molecules in Figures 3 and 4, respectively. The coordination geometry about nickel in both molecules is essentially square planar. N(1) and N(3) are raised slightly (0.057 (16) Å) out of the least-squares plane defined by the 24 macrocycle atoms of the general position molecule. The twofold axis that produces the disordered arrangement is contained in the mean macrocycle plane of the special position molecule (see Figure 2). Additionally, the NiN_4 core of this molecule is coplanar with the macrocycle plane within experimental error.

The general position molecule has a rather small but real distortion from planarity. The symmetry of the macrocycle approaches D_{2d},[36] but not by the S_4 ruffling usually associated with this symmetry.[34] In this case, dihedral mirror planes bisect opposite C_b–C_b bonds. The pattern of deviations is like that of C_{4v}-domed porphyrins, except that alternate pyrrole rings are above *and* below the mean macrocycle plane. Only one methine carbon atom is more than three standard deviations from the plane of the macrocycle. The average and maximum absolute value of the deviations of the 20 macrocycle carbons from the plane are 0.09 (2) and 0.21 (2) Å, respectively. The special position molecule is significantly more distorted from planarity, but in a different manner than the general position molecule. The special position macrocycle is S_4 ruffled in the conventional fashion; the dihedral mirror planes[36] contain the S_4 axis and opposite pairs of methine carbon atoms. The methine carbons have the largest displacements of any macrocycle atom from the mean plane, alternating 0.36 Å above and below. The average and maximum absolute value of the deviations of the 20 macrocycle carbons of the special position molecule from the plane are 0.22 (3) and 0.37 Å, respectively.

An unexpected feature of the structure is apparent in Figures 1 and 3. For the general position molecule, all of the ethyl groups, excluding the *gem*-diethyl group, are directed to one side of the molecule. This is clearly not the case for the special position

---

(35) Ulman, A.; Gallucci, J.; Fisher, D.; Ibers, J. A. *J. Am. Chem. Soc.* **1980**, *102*, 6852.

(36) The symmetries discussed here are idealized for a macrocycle with four equivalent pyrrole rings. Actual symmetries are lower.

molecule, as seen in Figures 2 and 4. A partial packing diagram of the general position molecule and two inversion related molecules is shown in Figure 5. In this case, there is some evidence for weak π–π overlap (intermolecular contacts of 3.4–3.6 Å), with each "end" of the molecule overlapping slightly. Strong overlap is prevented by the presence of the *gem*-diethyl group, as seen in the figure. The extent of overlap is too small to suggest that π–π interactions play a major role in the near planarity of the general position molecule. The special position molecule does not interact with other molecules in this manner. It is interleaved in the packing arrangement at an angle of 67° to the general position molecule. There is no evidence of intermolecular interactions between the carbonyl oxygen atom and any Ni atoms.

The most striking structural feature of nickel hydroporphyrin complexes is their extreme nonplanarity.[35,37,38] The core sizes of planar porphyrin and hydroporphyrin complexes are larger than that which would result in optimal Ni–N bond lengths.[37,39] Ni(OEP) crystallizes in two polymorphic forms: the planar triclinic form[40] has an average Ni–N distance of 1.958 (2) Å while the S_4-ruffled tetragonal form[41] has an average Ni–N distance of 1.929 (3) Å and a displacement of methine carbons 0.51 Å above and below the macrocycle plane. The existence of two crystalline forms has been taken as evidence for a delicate balance between (a) maximum π-delocalization, which favors planarity, (b) optimization of Ni–N bond lengths, which favors S_4 ruffling, and (c) crystal packing forces.[42] Structures of nickel hydroporphyrins have invariably revealed marked S_4 ruffling. The extent of ruffling has been observed to increase with increasing saturation of the π-system. By way of example, Ni(TMC) has an average Ni–N distance of 1.926 (5) Å and mean and maximum deviations from the 24-atom best plane are 0.29 and 0.60 Å, respectively, whereas Ni(TMiBC) has an average Ni–N distance of 1.919 (7) Å and mean and maximum deviations of 0.35 and 0.78 Å, respectively.[37] The extent of distortion of nickel hydroporphyrin complexes has been attributed to optimization of Ni–N bond lengths permitted by the increased flexibility of hydroporphyrins (owing to their decreased aromaticity).[37,39] The argument has been extended to suggest that hydroporphyrins are more conformationally labile and the structural differences between the different ligation and spin states of iron hydroporphyrin complexes will be small,[39] factors that may be significant in the biological roles of hydroporphyrins.

The existence of two conformations of Ni(**5**) in the same lattice with rather different extents of deviation from planarity resembles the two polymorphs of Ni(OEP). However, the degree of ruffling in the special position Ni(**5**) is significantly smaller and the Ni–N distances larger than in tetragonal Ni(OEP). The ease of deformation of the monooxoporphyrin macrocycle would appear to be comparable to or perhaps smaller than that of a porphyrin macrocycle. Thus, although **5** is formally analogous to a chlorin, the present results suggest that it is somewhat less flexible. Conjugation of the carbonyl to the π-system of the macrocycle could compensate for the decrease in aromaticity resulting from removal of the C_b–C_b double bond. Evidence for conjugation of the carbonyl is provided by NMR and electrochemical data. More detailed comparisons of oxoporphyrin and hydroporphyrin conformations will require further investigation.

Reactivity at the Oxoporphyrin Periphery. The oxime derivative of the monooxoporphyrin complex obtained from etioporphyrin I has been prepared in a reported yield of 23%.[14] The change from a *gem*-methyl and *gem*-ethyl adjacent to the carbonyl in the etioporphyrin complex to a *gem*-diethyl group in H_2(**5**) was sufficient to prevent reaction. Greater than 95% recovery of starting H_2(**5**) was observed under identical reaction conditions. Attempts to prepare thioketal derivatives of H_2(**5**) by reaction with ethane- or propanedithiol and $BF_3{\cdot}OEt_2$[43] lead only to formation of $H_3(\mathbf{5})^+$. Hydrazones of H_2(**5**) were neither isolable nor formed in situ to any appreciable extent. The latter is evidenced by the nearly quantitative recovery of H_2(**5**) when it is subjected to the Huang-Minlon modification of the Wolff–Kishner reaction[44] (hydrazine, potassium hydroxide, and diethylene glycol refluxed at 200 °C).

Alkyllithium reagents add to the keto group of H_2(**5**).[8,12] The reactions of H_2(**5**) with other metal alkyl reagents were examined to determine the generality of this reactivity. Trimethylaluminum has been reported to exhaustively C-methylate ketones at elevated temperatures.[45] Reaction of H_2(**5**) and trimethylaluminum at room temperature resulted in the immediate formation of a green complex. The metalloporphyrin-like UV–vis spectrum, the presence of O—H and C═O bands in the IR spectrum, and the similarity of the ^{1}H NMR spectrum of this complex and of H_2(**5**) permits its identification as Al(**5**)OH. Metalation of H_2(OEP) by organoaluminum reagents has been demonstrated previously.[24,46] At least five major products were obtained when the above reaction was carried out at elevated temperature. None had UV–vis spectral typical of porphyrins or metalloporphyrins. The absence of a carbonyl band in the IR spectra of these complexes suggested that the keto group had been reduced. Characterization of these products was not attempted. The reaction of H_2(**5**) with CH_3MgBr gave similar results. The magnesium complex of H_2(**5**) formed immediately upon mixing. No further reaction was noted, even when a great excess of CH_3MgBr was added.

Reactions of H_2(**5**) and hydride reagents have not been reported. We found the keto group inert toward sodium borohydride and Aldrich L-Selectride. Lithium triethylborohydride reacted sluggishly with H_2(**5**) to give a green product, **11**, identified as 2-hydroxy-3,3,7,8,12,13,17,18-octaethylchlorin. The UV–vis spectrum of **11** was nearly identical with respect to the number and relative intensity of bands to the spectrum of H_2(OEC).[47,48] Slight differences in the spectra included a 1–5-nm blue shift of the visible bands and a significantly greater ratio of the intensity of the Soret band to the 642-nm band in **11** relative to H_2(OEC). The carbonyl band characteristic of oxoporphyrins was absent from the IR spectrum of **11**. Two new bands were observed: one assignable to an O–H stretch and a second at 1615 cm^{-1}. The latter is a characteristic frequency of the chlorin macrocycle.[10,49]

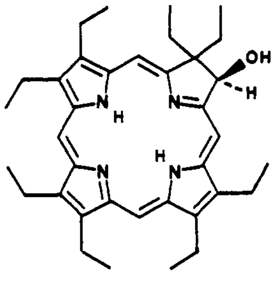

H_2(**11**)

---

[37] Suh, M. P.; Swepston, P. N.; Ibers, J. A. *J. Am. Chem. Soc.* **1984**, *106*, 5164.

[38] Kratky, C.; Angst, C.; Johansen, J. E. *Angew. Chem., Int. Ed. Engl.* **1981**, *20*, 211.

[39] Strauss, S. H.; Silver, M. E.; Ibers, J. A. *J. Am. Chem. Soc.* **1983**, *105*, 4108.

[40] Cullen, D. L.; Meyer, E. F., Jr. *J. Am. Chem. Soc.* **1974**, *96*, 2095.

[41] Meyer, E. F., Jr. *Acta Crystallogr., Sect. B: Struct. Crystallogr. Cryst. Chem.* **1972**, *B28*, 2162.

[42] Hoard, J. L. *Ann. N.Y. Acad. Sci.* **1973**, *206*, 18.

[43] Fieser, L. F. *J. Am. Chem. Soc.* **1954**, *76*, 1945.

[44] Huang-Minlon. *J. Am. Chem. Soc.* **1949**, *71*, 3301.

[45] Meisters, A.; Mole, T. *J. Chem. Soc., Chem. Commun.* **1972**, 595; *Aust. J. Chem.* **1974**, *27*, 1655.

[46] Buchler, J. W.; Puppe, L.; Schneehage, H. H. *Justus Liebigs Ann. Chem.* **1971**, *749*, 134.

[47] Whitlock, H. W., Jr.; Hanauer, R.; Oester, M. Y.; Bower, B. K. *J. Am. Chem. Soc.* **1969**, *91*, 7485.

[48] Reference 17 notes that the UV–vis spectra of more than 20 natural and synthetic chlorins are "remarkably homogeneous in that the overall pattern is relatively unaffected by electronic effects".

[49] Golden, J. H.; Linstead, R. P.; Whitham, G. H. *J. Chem. Soc.* **1956**, 1725. Wetherell, H. R.; Hendrickson, M. J.; McIntyre, A. R. *J. Am. Chem. Soc.* **1959**, *81*, 4715. Burger, H.; Burczyk, K.; Buchler, J. W.; Furhop, J. H.; Hofler, F.; Schrader, B. *Inorg. Nucl. Chem. Lett.* **1970**, *6*, 171.

The oxidations and reductions of **11** (see below) occur at potentials that are quite similar to those of H_2(OEC) but rather different than those of H_2(**5**).

^{1}H NMR and mass spectroscopic evidence further corroborate the indentification above. The methine protons of H_2(**5**) are found at 9.94, 9.86, 9.83, and 9.12 ppm. The upfield peak has been assigned to the methine proton adjacent to the *gem*-diethyl group.[8] The proton at 9.94 ppm is the one most shifted and broadened by addition of Eu(fod)$_3$, suggesting that it is adjacent to the keto group and is deshielded by it. The methine region in **11** is more typical of a chlorin, with protons at 9.77, 9.75, 9.18, and 8.77 ppm as compared with 9.71 and 8.87 ppm in the more symmetric H_2(OEC).[31] Two complicated multiplet patterns are observed between 2.2 and 2.7 ppm. Two peaks on the lowfield side of the lowfield multiplet and an integrated intensity of one proton are lost upon exchange with D_2O. The peaks can be assigned to the hydroxy proton. A doublet at 6.53 ppm collapses to a singlet upon exchange; it is assigned to the β-proton on the reduced ring. The 2 ppm shift downfield of this proton relative to the 7,8-protons in H_2(OEC) is attributed to the effect of the *gem*-hydroxy group. The methyl protons of the *gem*-diethyl groups have two distinct chemical shifts that are substantially downfield from the *gem*-diethyl methyl protons in H_2(**5**) but are approaching the expected value in H_2(OEC). Simultaneous irradiation of both methyl triplets permits assignments of the two multiplets between 2.2 and 2.7 ppm to the methylene protons of the *gem*-diethyl groups. The multiplets collapse to two overlapping AB quartets with substantially different chemical shift differences between their A and B protons. These observations are fully consistent with the expected shifts and coupling in the reduced ring of 2-hydroxy-3,3,7,8,12,13,17,18-octaethylchlorin. Finally, the parent ion peak of H_2(**11**) is observed at *m/e* 552 and a peak corresponding to loss of water at 534. The latter peak is not observed in the mass spectra of complexes of oxoporphyrin **5**.

The keto group of H_2(**5**) is also reduced by $LiAlH_4$, but this hydride metalates the macrocycle as well.[50] There are two possible isomers of Al(**11**)OH; one with the macrocycle and aluminum axial OH groups on the same side of the macrocycle and the other with the OH groups on opposite sides. As expected, two products with similar UV-vis spectra can be isolated from the crude reaction product. Insufficient quantities of the minor product were obtained to permit further characterization. The IR of the major product lacked a carbonyl band and had the expected OH and chlorin bands. The ^{1}H NMR spectrum was rather broad (inter- and intramolecular hydrogen bonding is possible; see below), but the methine protons were resolved. Their shifts are similar but somewhat upfield from the values observed for H_2(**11**).

Overall, the monooxoporphyrin H_2(**5**) is remarkably inert and stable toward reagents that are reactive with carbonyl groups. The inertness toward addition of all but lithium reagents to the carbonyl group suggests that formation of a tetrahedral carbon is rather energetically disfavored. Both steric crowding and loss of conjugation with the oxoporphyrin π-system may deactivate the carbonyl toward addition, except in those cases where a strong alkoxide–alkali-metal interaction results.

Voltammetry. The redox properties of free-base and metal complexes of porphyrins[51,52] and hydroporphyrins[18,52-58] have been extensively investigated and are well understood. The redox properties of oxoporphyrins have not been examined. An electrochemical study has been undertaken to define the primary redox processes of free-base mono- and dioxoporphyrins and selected metal complexes of the former. Potentials are collected in Table V.

Table V. Potentials of Free-Base Oxoporphyrin and Metallooxoporphyrin Complexes

	$E_{1/2}$,^{a} V			
complex	$2^+/1^+$	$1^+/0$	$0/1^-$	$1^-/2^-$
H_2(**5**)	1.24	0.86	−1.23	−1.73
H_2(**6**)	1.33^b	0.83	−1.13	−1.57
H_2(**7**)	1.27^b	0.82	−1.00	−1.51
H_2(**9**)	1.27	0.82	−1.06	−1.66
H_2(**10**)	1.25	0.83	−1.14	−1.67
Cu(**5**)	1.27	0.73	−1.25	−1.85
Mg(**5**)	0.81	0.51	−1.56^c	
Ni(**5**)	0.92	0.76	−1.19	−1.96^c
Zn(**5**)	0.95	0.60	−1.38	−1.82
H_2(**11**)^d	1.18^b	0.68	−1.43	−1.96^c

^{a} $E_{1/2} = {}^1/_2(E_{p,a} + E_{p,c})$; at 25 °C vs. SCE in acetonitrile solution 0.1 M in TBAP. ^{b} $E_{p,a}$ (irreversible). ^{c} $E_{p,c}$ (irreversible). ^{d} Literature data for H_2(OEC) 1.11, 0.59, −1.46, −1.9 V.[31]

Typical of most porphyrins[51,52] and hydroporphyrins,[31,54,55] free-base mono- and dioxoporphyrins undergo two one-electron oxidations to cation radicals and dications and two one-electron reductions to anion radicals and dianions. The first oxidations and reductions conform closely to strict reversibility criteria, especially if scanned separately. With the exception of the isobacteriochlorin analogues H_2(**6**) and H_2(**7**), second oxidations and reductions of oxoporphyrins are chemically but not electrochemically reversible. The second reduction of H_2(**6**) is chemically reversible, but the second oxidation is chemically irreversible at scan speeds as high as 1000 mV/s. The second oxidation and reduction of H_2(**7**) are chemically irreversible at scan speeds as high as 1000 mV/s.

The potential of the first oxidation of H_2(**5**) is shifted approximately 30 mV negative of the first oxidation of H_2(OEP)[31] The potentials of the first oxidations of all isomeric free-base dioxoprophyrins fall within a 20-mV range whose center is only 40 mV negative of the first oxidation of H_2(**5**). Similar trends pertain for the second oxidations except that the range of potentials for this process in the dioxoporphyrins is shifted about 40 mV positive of the potential for H_2(**5**). Quite different trends are noted for reduction processes. The first reduction of H_2(**5**) occurs 210 mV positive of the corresponding process for H_2(OEP). Furthermore, the potentials of the first reductions of dioxoporphyrins fall in a 140-mV range whose center is 170 mV positive of the first reduction of H_2(**5**). By way of comparison, the ease of oxidation of hydroporphyrins follows the series isobacteriochlorin > chlorin > porphyrin, with successive potential intervals of 250–300 mV.[31] Additionally, the ease of reduction follows the series porphyrin ≥ chlorin > isobacteriochlorin. Thus, the electrochemical behavior of free-base oxoporphyrins is distinctly different from that of porphyrins and hydroporphyrins. Conjugation of the oxoporphyrin π-system with a carbonyl group appears to compensate for the loss of a C_b–C_b double bond in the energy of the HOMO and substantially lowers the energy of the LUMO.

The potentials of the redox processes of the Cu, Mg, and Zn complexes of **5** are shifted negatively relative to the potentials of H_2(**5**) in a fashion parallel to the shifts observed upon metalation of H_2(OEP).[59] The oxidations of Ni(**5**) differ from those of Ni(OEP) in that there are two closely spaced one-electron oxidations rather than one two-electron oxidation. The two processes

---

(50) H_2(OEP) is metalated by $LiAlH_4$ under identical conditions. Reactions of H_2(**5**) and H_2(OEP) with $LiAlH_4$ appear to involve electron transfer, as evidenced by the series of color changes after exposure of the reaction mixture to air and the blackening of the Teflon stir bar. The later is also observed in reactions employing alkali metals in amine solutions. Ligand-based reduction of vanadyl octaethylporphyrin by $LiAlH_4$ has also been reported; see ref 60.

(51) Furhop, J. H. *Struct. Bonding (Berlin)* **1974**, *18*, 1.

(52) Felton, R. H. In "The Porphyrins"; Dolphin, D., Ed.; Academic Press: New York, 1978; Vol. 5, Chapter 3.

(53) Stolzenberg, A. M.; Spreer, L. O.; Holm, R. H. *J. Chem. Soc., Chem. Commun.* **1979**, 1077.

(54) Richardson, P. F.; Chang, C. K.; Spaulding, L. D.; Fajer, J. *J. Am. Chem. Soc.* **1979**, *101*, 7736.

(55) Richardson, P. F.; Chang, C. K.; Hanson, L. K.; Spaulding, L. D.; Fajer, J. *J. Phys. Chem.* **1979**, *83*, 3420.

(56) Chang, C. K.; Fajer, J. *J. Am. Chem. Soc.* **1980**, *102*, 848.

(57) Chang, C. K.; Hanson, L. K.; Richardson, P. F.; Young, R.; Fajer, J. *Proc. Natl. Acad. Sci. U.S.A.* **1981**, *78*, 2652.

(58) Fujita, E.; Fajer, J. *J. Am. Chem. Soc.* **1983**, *105*, 6743.

(59) Furhop, J. H.; Kadish, K. M.; Davis, D. G. *J. Am. Chem. Soc.* **1973**, *95*, 5140.

(60) Bonnet, R.; Brewer, P.; Noro, K.; Noro, T. *Tetrahedron* **1978**, *34*, 379.

Inorg. Chem. **1986**, *25*, 991–995

are expected to involve macrocycle oxidation and oxidation of Ni^{II} to Ni^{III}, in analogy with Ni(OEP),[59] but further investigation is required in order to make assignments. Unlike M(OEP), the second reductions of M(**5**) (except for M = Mg) are accessible. The first reduction of Mg(**5**) is chemically reversible only at scan speeds in excess of 200 mV/s.

The potentials of H_2(**11**) included in Table V are quite similar to those of H_2(OEC)[31] but differ significantly from those of H_2(**5**). The second oxidation of **11** is totally irreversible. After scanning through this wave, one observes a small unidentified reduction peak at 0.93 V (ECE process) but no reduction of $H_2(\mathbf{11})^{+\cdot}$. Loss of H^+ from the reduced ring β-carbon or from the hydroxyl group of $H_2(\mathbf{11})^{2+}$ are possible explanations of these observations. The former reaction is consistent with the behavior of β-hydrogenated hydroporphyrins.[31]

Conclusions. The results of this investigation of free-base β-oxoporphyrins and metallo-β-oxoporphyrins lead to the following conclusions:

(i) The oxoporphyrin structure type has been confirmed by X-ray structural means.

(ii) The conformations of Ni(**5**) in the solid state deviate from planarity to a lesser extend than those of nickel complexes of hydroporphyrins.

(iii) The carbonyl groups of oxoporphyrins are rather unreactive. Conjugation of the carbonyl to the macrocycle π-system and steric effects may contribute.

(iv) The potentials of the oxidations of oxoporphyrins are similar to those of porphyrins.

(v) The potentials of the reductions become progressively more positive than those of porphyrins and hydroporphyrins as more carbonyl groups are introduced.

(vi) Oxoporphyrins and hydroporphyrins are structurally, electronically, and chemically distinct.

Acknowledgment. We thank the Camille and Henry Dreyfus Foundation (A.M.S.), the Research Corp., the NIH (Grant BRSG S07 RR07044), and the Brandeis Undergraduate Research Program (P.A.G.) for support of this research and Dr. C. K. Chang for providing us with a preprint of ref 17.

Supplementary Material Available: Listings of thermal parameters and nonessential bond lengths (3 pages). Ordering information is given on any current masthead page. According to policy instituted Jan 1, 1986, the tables of calculated and observed structure factors (8 pages) are being retained in the editorial office for a period of 1 year following the appearance of this work in print. Inquiries for copies of these materials should be directed to the Editor.

Contribution from the Department of Chemistry,
University of Houston—University Park, Houston, Texas 77004

Ligand-Addition Reactions of Indium(III) Porphyrins. Reactions of (OEP)InX and (TPP)InX with *N*-Methylimidazole and Pyridine

J.-L. Cornillon, J. E. Anderson, and K. M. Kadish*

Received October 21, 1985

The reactions of *N*-methylimidazole (*N*-MeIm) and pyridine with (P)In(X), where P is either the dianion of octaethylporphyrin (OEP) or the dianion of tetraphenylporphyrin (TPP) and X is Cl^-, OAc^-, SO_3Ph^-, or $SO_3CH_3^-$, were monitored by ^1H NMR, electronic absorption spectroscopy, and conductivity measurements. All three methods were self-consistent in demonstrating the stepwise formation of hexacoordinated monomeric In–porphyrin species of the type (P)InX(L) and $[(P)In(L)_2]^+$, where L = pyridine or *N*-MeIm. Equilibrium constants for the ligand-addition reactions of (P)InX and (P)InX(L) were also calculated from the electronic absorption spectra. This is the first time that monomeric, hexacoordinated In(III) porphyrins have been reported.

Introduction

Indium(III) porphyrins of the type (P)InX[1-5] and (P)In(R)[6-9] have been characterized, where P is the dianion of tetraphenylporphyrin (TPP) or octaethylporphyrin (OEP), X is an anionic ligand, and R is one of several different σ-bonded alkyl or aryl groups. Bimetallic indium porphyrins of the form $(P)InM'(L)_n$ have also been reported, where $M'(L)_n$ is an axial ligand of the type $M(CO)_x(\eta^5\text{-}C_5H_5)_y$.[10,11] For the last series of compounds, the indium oxidation state is not known but bimetallic $(P)InW(CO)_3Cp$ has been postulated to contain In(I).[12]

In two recent papers we reported the electrochemistry of ionic[13] and σ-bonded[14] In(III) porphyrins in methylene chloride and benzonitrile. In these nonbonding solvents the In(III) atom is invariably five-coordinate. Six-coordinate In(III) complexes have been characterized in the solid state,[15-17] but such coordination has never been reported for monomeric In(III) porphyrins, which

---

(1) Buchler, J. W.; Eikelmann, G.; Puppe, L.; Rohbock, K.; Schneehage, H. H.; Weck, D. *Justus Liebigs Ann. Chem.* **1971**, *745*, 135.
(2) Bhatti, M.; Bhatti, W.; Mast, E. *Inorg. Nucl. Chem. Lett.* **1972**, *8*, 133.
(3) Eaton, S. S.; Eaton, G. R. *J. Am. Chem. Soc.* **1975**, *97*, 3660.
(4) Guilard, R.; Cocolios, P.; Fournari, P.; Lecomte, C.; Protas, J. *J. Organomet. Chem.* **1979**, *168*, C49.
(5) Cocolios, P.; Fournari, P.; Guilard, R.; Lecomte, C.; Protas, J.; Boubel, J. C. *J. Chem. Soc., Dalton Trans.* **1980**, 2081.
(6) Cocolios, P.; Guilard, R.; Fournari, P. *J. Organomet. Chem.* **1977**, *129*, C11.
(7) Cocolios, P.; Guilard, R.; Fournari, P. *J. Organomet. Chem.* **1979**, *179*, 311.
(8) Lecomte, C.; Protas, J.; Cocolios, P.; Guilard, R. *Acta Crystallogr., Sect. B: Struct. Crystallogr. Cryst. Chem.* **1980**, *B36*, 2769.
(9) Cocolios, P.; Guilard, R.; Bayeul, D.; Lecomte, C. *Inorg. Chem.* **1985**, *24*, 2058.
(10) Cocolios, P.; Moise, C.; Guilard, R. *J. Organomet. Chem.* **1982**, *228*, C43.
(11) Onaka, S.; Yamashita, M.; Tatematsu, Y.; Kato, Y.; Goto, M.; Ito, T. *Inorg. Chem.* **1985**, *24*, 1070.
(12) Cocolios, P.; Chang, D.; Vittori, O.; Guilard, R.; Moise, C.; Kadish, K. M. *J. Am. Chem. Soc.* **1984**, *106*, 5724.
(13) Kadish, K. M.; Cornillon, J.-L.; Cocolios, P.; Tabard, A.; Guilard, R. *Inorg. Chem.* **1985**, *24*, 3645.
(14) Kadish, K. M.; Boisselier-Cocolios, B.; Cocolios, P.; Guilard, R. *Inorg. Chem.* **1985**, *24*, 2139.
(15) Contreras, J. G.; Einstein, F. W.; Gilbert, M. M.; Tuck, D. G. *Acta Crystallogr., Sect. B: Struct. Crystallogr. Cryst. Chem.* **1977**, *B33*, 1648.
(16) Wignacourt, J. P.; Mairesse, G.; Barbier, P. *Cryst. Struct. Commun.* **1976**, *5*, 293.
(17) Whithow, S. M.; Gabe, E. J. *Acta Crystallogr., Sect. B: Struct. Crystallogr. Cryst. Chem.* **1975**, *B31*, 2534.

0020-1669/86/1325-0991$01.50/0 © 1986 American Chemical Society